Original Article

Possible Protective Role of Pirfenidone Versus Combined Antifibrotic Therapy Colchicine and Pirfenidone in a Rat Model of Bleomycin Induced Pulmonary Fibrosis and Evaluation of their Potential Impact on α-SMA, IL6 and TGFβ (Histological and Immunohistochemical Study)

Walaa Adel Abdelmoez

Department of Anatomy and Embryology, Faculty of Medicine, Ain Shams University, Egypt

ABSTRACT

Introduction: Combined antifibrotic treatment strategy in the management of pulmonary fibrosis attracts the attention worldwide especially after COVID-19 pandemic and still a point of recent research work.

Aim of the Work: This study intended to clarify the possible protective serve of Pirfenidone only versus combined antifibrotic action of both pirfenidone and colchicine in a bleomycin created pulmonary fibrosis rat model.

Materials and Methods: Forty adult albino male rats were partitioned equally into four groups. Control group I. Bleomycin-treated group II: (10mg/kg/d by intraperitoneal injection for the first 5 days of the experiment). Pirfenidone-treated group III: (100mg/kg/d orally). Combined pirfenidone and colchicine-treated group IV: (oral pirfenidone 100mg/kg/d + oral colchicine 0.5mg/kg/d for 30 days in the created pulmonary fibrosis model).

Results: Histopathological results of group II revealed marked distortion of the bronchiolar mucosal lining and the alveolar system. Mast cells appeared infiltrating the pulmonary interstitium. Multiple lamellar bodies appeared in pneumocyte type I and II. Moreover, the myofibroblasts appeared in large number in the interalveolar septa. There was significant increase in the immune staining areas of both α-SMA, IL6 and the collagen deposition between group II and group I. Dramatic rise in serum concentrations of TGβ, IL6, MDA and SOD compared to the control group. Group III showed moderate improvement of histopathological and immunohistochemical findings as well as the collagen deposition and serum inflammatory markers were decreased significantly between groups III and II. The best results were observed in group IV, a significant fall in the immunostaining areas of both α-SMA and IL6 and marked decrease of serum levels of SOD and MDA levels between group IV and groups III and II.

Conclusion: Combined antifibrotic therapy offered remarkable improvement in the architecture of the pulmonary tissue. There was substantial improvement in the histopathological and immunohistochemical features in the combined group in comparison with pirfenidone treated group.

INTRODUCTION

Idiopathic pulmonary fibrosis (IPF) is deadly interstitial lung disorder[1,4]. Great attention is directed toward understanding its pathogenesis and possible treatment strategies especially after COVID-19 pandemic[30]. There is a great concern about the role of Interleukin (IL6) and alpha smooth muscle actin (α-SMA) in the etiology of pulmonary fibrosis. Interleukin-6 is proinflammatory cytokine, which is produced by numerous types of cells[23]. It can promote fibrosis by creating severe inflammatory reaction through activation of TGFβ pathway[28]. In fibrosis condition; there is an emergence of activated myofibroblasts which are characterized by α-SMA expression. Increased α-SMA expression is thought to be responsible for increased contractility of the affected tissues, marked increase in collagen expression and extracellular matrix deposition[3]. Moreover, alpha smooth muscle actin may be possible

contributor to the pathogenesis of pulmonary fibrosis, and its suppression may decrease the fibrotic process and improve the symptoms of patients.

A TGFβ-synthesis inhibitor with an anti-inflammatory and antioxidant properties is pirfenidone[25]. It can lessen fibroblast proliferation, collagen deposition, and alpha smooth actin (α-SMA) expression. As a result, it can shield pneumocytes from the destructive effect of the cytokine storm[10]. Numerous clinical studies are still looking for ways to enhance the therapeutic impact of pirfenidone in the treatment of IPF[8,16]. On other hand, Colchicine inhibits fibroblast proliferation and collagen synthesis effectively[2]. Previous researches demonstrated that colchicine could inhibit a variety of leukocyte functions. IL-6, TNF-α, IL-4 and transforming growth factor-β are cytokines that are known to be essential for fibrogenesis. The potential effect of colchicine on the previously mentioned cytokines and

on the oxidative stress markers still a vague issue. From a clinical standpoint, colchicine is the agent of choice for combined therapeutic strategies regarding treatment of pulmonary fibrosis[22].

MATERIALS AND METHODS

Ethical approval

The research was certified by the Ain Shams University Ethical Committee, with approval number FWA 000017585.All study procedures were done in accordance with the guidelines of (CARE). The local Ethics committee of Medical School-Ain Shams University.

Experimental drugs

1. **Bleomycin (Bleocare®15):** bleomycin lyophilized powder 15 units for intraperitoneal injection, handled in saline solution and purchased from RMPL PHARMA LLP. (Mumbai, Maharashtra, India).

2. **Pirfenidone (pirfenex®200mg):** pirfenex 200mg powder handled in saline solution and purchased from Cipla Ltd pharma company. Mumbai, Maharashtra, India).

3. **Colchicine (Colchicine®0.5mg):** colchicine 0.5 mg powder, dissolved in normal saline and purchased from El-Nasr pharmaceuticals company (Gesr El Suez, Cairo, Egypt).

Experimental design & Procedures

Forty adult male albino rats weighing 150-200 g were divided equally into 4 groups. They were housed in cages made of stainless steel, with two rats per cage and a 30x35cm size. The study excluded rats that were afflicted with a disease, had been used in previous experiments, had difficult walking, or had poor fur. The rats were exposed to suitable environmental conditions and ventilation.

Group I (control): received 1ml normal saline by oral gavage every day for 30 successive days.

Group II (Bleomycin-treated group): received 10mg/kg/d bleomycin dissolved in 1ml normal saline by intraperitoneal injection for 5 consecutive days; the first five days of the experiment.

Group III (Bleomycin+Pirfenidone-treated group): received 10mg/kg/d bleomycin dissolved in 1ml normal saline by intraperitoneal injection for 5 consecutive days; the first five days of the experiment+ Pirfenidone100mg/kg/d dissolved in 1ml normal saline and given by oral gavage from day 1 to day 30.

Group IV (combined Bleomycin + Pirfenidone + colchicine-treated group): received 10mg/kg/d bleomycin dissolved in 1ml normal saline by intraperitoneal injection for 5 consecutive days; the first five days of the experiment+ Pirfenidone 100mg/kg/d dissolved in 1ml normal saline and given by oral gavage + colchicine 0.5mg/kg/d dissolved in 1ml normal saline and given by oral gavage. Both drugs

were administered orally from day (1), the day of the first bleomycin injection and they were continuous to day (30). The drugs were given till the end of the experiment.

Tissue sampling

At the end of the experimental period (30 days), rats were rendered unconscious with an intraperitoneal injection of ketamine (90 mg/kg)+xylazine (15 mg/kg) and afterwards sacrificed. Lung tissue samples were dissected and obtained for histopathological and immunohistochemical investigation.

Histological and immunohistochemical techniques

For light microscopic examination

Lung samples were dissected, fixed in 10% neutral formalin for ten days, and processed into paraffin blocks. Blocks of paraffin were sliced around 5-7 μ thick and stained with Hematoxylin and Eosin (H&E) and Masson's Trichrome stain.

For immunohistochemistry

For immunohistochemical staining, sections were deparafinized, rehydrated and rinsed in phosphate-buffered saline (PBS). The sections were then stored in a blocking solution (10% normal goat serum) for 60 minutes at room temperature (22°C). The secondary antibodies were then treated with Interleukin-6 (IL-6), a mouse monoclonal antibody (1:400; Elabscience biotechnology, USA), and alpha smooth muscle actin (α-SMA), a rabbit polyclonal antibody (1:100; Elabscience biotechnology, USA). After PBS, the sections were incubated at room temperature for 20 minutes with a biotinylated secondary antibody. After washing with PBS, slices were exposed for 10 minutes to a Streptavidin-Horseradish peroxidase solution. For secondary antibody binding, 3,3-diaminobenzoic acid diluted in PBS was utilized, and 0.03% H_2O_2 was added before to use. After dipping the sections in PBS, two drops of hematoxylin were used to counterstain the slides.

For electron Microscopic study

The standard protocol for processing lung tissue samples for transmission electron microscopy was followed. fragments of lung tissue were fixed for 2 hours in 2.5% phosphate- buffered glutaraldehyde at 4°C were followed by rinsing in phosphate- buffered saline. Lung specimens were then post-fixed in 1% prepared phosphate buffer osmium tetroxide at 4°C for one hour. The lung samples were then dehydrated in ascending alcohol concentrations, submerged in propylene oxide and encapsulated in an epoxy resin mixture. 1 μm semithin slices were cut, stained with toluidine blue and investigated by L/M to select the appropriate regions. To examine ultrathin sections (80-90 nm thick), uranyl acetate and lead citrate were used to create contrast[12]. The slices were viewed with a transmission electron microscope (TEM) ("Jeol" E.M.-100 CX11; Japan) at Ain Shams University's Electron Microscopic Unit.

For biochemical analysis

Blood samples were left to coagulate for 10 minutes before being centrifuged at 4,000 rpm. Using ELISA kits, the gathered serum was tested for levels of IL6 and TGFβ (E-EL-R0015, Elabscience Biotechnology, USA) and (E-EL-R1015, Elabscience Biotechnology, USA), respectively, in order to evaluate the inflammatory condition. To analyse the oxidative stress state, oxidative stress markers such as Superoxide dismutase (SOD) and Malonaldhyde dehydrogenase (MDA) were measured using ELISA kits no. E-BC-K025-S (Elabscience Biotechnology, USA) and E-BC-K020 (Elabscience Biotechnology, USA).

Morphometric study

These measurements were taken in Histology and Cell Biology Department of Faculty of Medicine, Ain Shams University, using the image analyzer (Image J application). Seven fields from seven independent serial sections containing seven animals from each group were used to calculate the area % of the immunological staining. The percentage of positively stained region in relation to the total lung tissue area was used to quantify the expression of IL-6, α-SMA and collagen deposition in the interalveolar septa.

Statistical analysis

The information gathered was provided as mean SD. SPSS version 23 was utilized for data analysis. Using one-way analysis of variance (ANOVA) and the Bonferroni post-hoc test, the significance of differences between groups was determined. When the *P-value* was less than 0.05, the result was judged statistically significant.

RESULTS

Histopathological results

Examining sections of the control group(I) stained with H&E and toluidine blue under a light microscope revealed the lung tissue consisting of respiratory bronchioles, alveolar ducts and saccules. The alveoli appeared separated from each other by thin alveolar septa(Figures 1A,6A). In addition, in H&E stained sections; the intrapulmonary bronchioles appeared composed of: mucosa, submucosa and adventitial layer (Figure 2A). The higher magnification revealed the epithelial lining of the mucosal layer consisting of basal cells, intermediate and goblet cells, as well as the Clara secretory cells also could be detected. Moreover, the lamina propria appeared thin and contains collagenous fibers with few cellular elements (Figure 3A). Besides, the submucosal blood vessels appeared with intact wall and endothelial lining (Figure 4A). Masson's trichrome stained sections revealed the normal collagen deposition in the interalveolar septa (Figure 5A). Transmission electron micrographs of the control group I showed patent alveolar lumen (AL) with thin interalveolar septa; the alveolar lumen appeared lined with type I pneumocyte with euchromatic nucleus and typeII pneumocyte with hemogenus layer of surfactant near its luminal surface (Figures 9 a,b,c).

In bleomycin treated group(II); the H&E stained sections revealed marked destruction of the normal lung architecture which appeared with distorted alveolar walls, thickened alveolar septa (Figure 1B) and disrupted bronchiolar wall with mononuclear inflammatory cell infiltrate (Figure 2B). The higher magnification revealed marked distortion of the mucosal epithelial lining down to the level of the basement membrane with extensive inflammatory cell infiltrate in the submucosal layer (Figure 3B). In addition, the submucosal blood vessels appeared markedly dilated with thinned wall and distorted epithelial lining (Figure 4B). Masson's trichrome stained sections revealed extensive collagen deposition in the pulmonary parenchyma (Figure 5B). Toluidine blue stained sections revealed extensive invasion of the mast cells to the pulmonary interstitium and interalveolar septa (Figure 6B). Electron micrographs of bleomycin treated groupII showed ruptured pneumocyte and released microparticles in the alveolar lumen, multiple lysosomal bodies and laminated inclusion bodies appeared near its luminal surface. Thickened alveolar septa, heavy collagen deposition multiple myofibroblasts and inflammatory cell infiltrate appeared in the pulmonary interstitium (Figures 9 d,e,f).

On other hand, in pirfenidone- treated group (III); there was apparent restoration of normal alveolar system and the bronchiolar wall appeared with intact mucosal lining (Figures 1C,2C). The higher magnification revealed apparent restoration of the normal epithelial lining of the bronchiolar mucosa and moderate reduction of the inflammatory cell infiltrate in the submucosal layer (Figure 3C). Moreover, the submucosal blood vessels appeared dilated, engorged with distorted endothelial lining (Figure 4C). Masson's trichrome stained sections revealed intense collagen deposition in the pulmonary interstitium (Figure 5C). Toluidine blue stained sections revealed mast cells still infiltrating the pulmonary parenchyma (Figure 6C). Pirfenidone treated group III showed thickened alveolar septa with myofibroblasts and macrophages invading it. Heavy collagen deposition appeared in the pulmonary parenchyma and inclusion bodies in the cytoplasm of pneumocyte (Figures 9 g,h,i).

Furthermore, the best results were observed in the combined group (IV); as there was apparent restoration of the normal lung architecture; the alveoli, alveolar septa and sacs. The bronchiolar wall appeared with intact mucosal epithelial lining with no inflammatory cell infiltrate (Figures 1D,2D,3D) with evident improvement in the submucosal blood vessels (Figure 4D). In addition, there was apparent restoration of the normal collagen distribution in the pulmonary interstitium (Figure 5D) and marked reduction of the number of mast infiltrating the pulmonary parenchyma (Figure 6D). Electron micrographs of group IV showed patent alveolar lumen, the interalveolar septum still invaded by inflammatory cells and myofibroblasts. Decreased number of inclusion bodies, proliferating nuclei, apical microvilli were clearly observed (Figures 9 j,k,l).

Results of immunohistochemistry

The immunohistochemical stained sections of the control group showed only few cells expressing the α-SMA the reaction appeared as granular brownish staining of the fibromyocytes (Figure 7A). Marked increase of the α-SMA expressing cells in the alveolar septa, in the peribronchial region and around the blood vessels appeared in bleomycin-treated group (Figure 7B). In pirfenidone-treated group there was marked decrease of the α-SMA expressing cells in the alveolar septa but still markedly observed in the bronchial wall and in the smooth muscles of the blood vessels (Figure 7C). Marked decrease in the immune-staining positive cells was observed in the combined group (Figure 7D).

IL6 immune-stained sections revealed very weak reaction in the control group appeared as mild brownish granular staining in the pulmonary interstitium (Figure 8A). In bleomycin-treated group marked increase in the expression of IL6 was clearly observed (Figure 8B). Moderate immune reaction to IL6 was clearly observed in pirfenidone- treated group (Figure 8C). In contrast, the combined group showed minimal immune reaction to IL6 (Figure 8D).

Morphometric and Statistical Results

Mean area % of IL6 in the pulmonary interstitium (Table 1, Histogram 1)

Compared to the other groups, group II showed a significant increase in the mean area% stained with IL6 with based on the data presented in table1. Group III demonstrated a significant decrease relative to group II, but a significant increase relative to groups I and IV. Group IV demonstrated a significant decrease relative to groups II and III, but a significant increase relative to group I.

Mean area % of α-SMA in the pulmonary interstitium (Table 2, Histogram 2)

Compared to other groups, group II showed a significant increase in the mean area % of α-SMA based on the data presented in table 2. Group III demonstrated a significant decrease relative to group II, but a significant increase relative to groups I and IV. Group IV demonstrated a significant decrease relative to groups II and III, but a significant increase relative to group I.

Mean area % of collagen distribution in the pulmonary interstitium (Table 3, Histogram 3)

Compared to other groups, group II showed a significant increase in the mean area % of collagen deposition with based on the data presented in table 3. Group III demonstrated a significant decrease relative to group II, but a significant increase relative to groups I and IV. Group IV demonstrated a significant decrease relative to groups II and III, but a significant increase relative to group I.

Statistical results of IL6 levels in rat serum (Table 4, Histogram 4)

Compared to other groups, group II showed a highly significant increase in the serum level of IL6 based on the data presented in table 4. Group III demonstrated a highly significant decrease relative to group II, but a highly significant increase relative to groups I and IV. Group IV demonstrated a highly significant decrease relative to groups II and III, but a highly significant increase relative to group I.

Statistical results of SOD levels in rat serum (Table 5, Histogram 5)

Compared to other groups, group II showed a highly significant increase in the serum level of SOD with based on the data presented in table 5. Group III demonstrated a highly significant decrease relative to group II, but a highly significant increase relative to groups I and IV. Group IV demonstrated a significant decrease relative to groups II and III, but a significant increase relative to group I.

Statistical results of MDA levels in rat serum (Table 6, Histogram 6)

Compared to other groups, group II showed a highly significant increase in the serum level of MDA with based on the data presented in table 6. Group III demonstrated a highly significant decrease relative to group II, but a highly significant increase relative to groups I and IV. Group IV demonstrated a significant decrease relative to groups II and III, but a significant increase relative to group I.

Statistical results of TGβ levels in rat serum (Table 7, Histogram 7)

Compared to other groups, group II showed a highly significant increase in the serum level of TGβ based on the data presented in table 7. Group III demonstrated a highly significant decrease relative to group II. No statistical significant difference between groups I and IV. Group IV demonstrated a highly significant decrease relative to groups II, but no statistical significant difference between groups IV and I, III. A highly statistical significant decrease relative to group II.
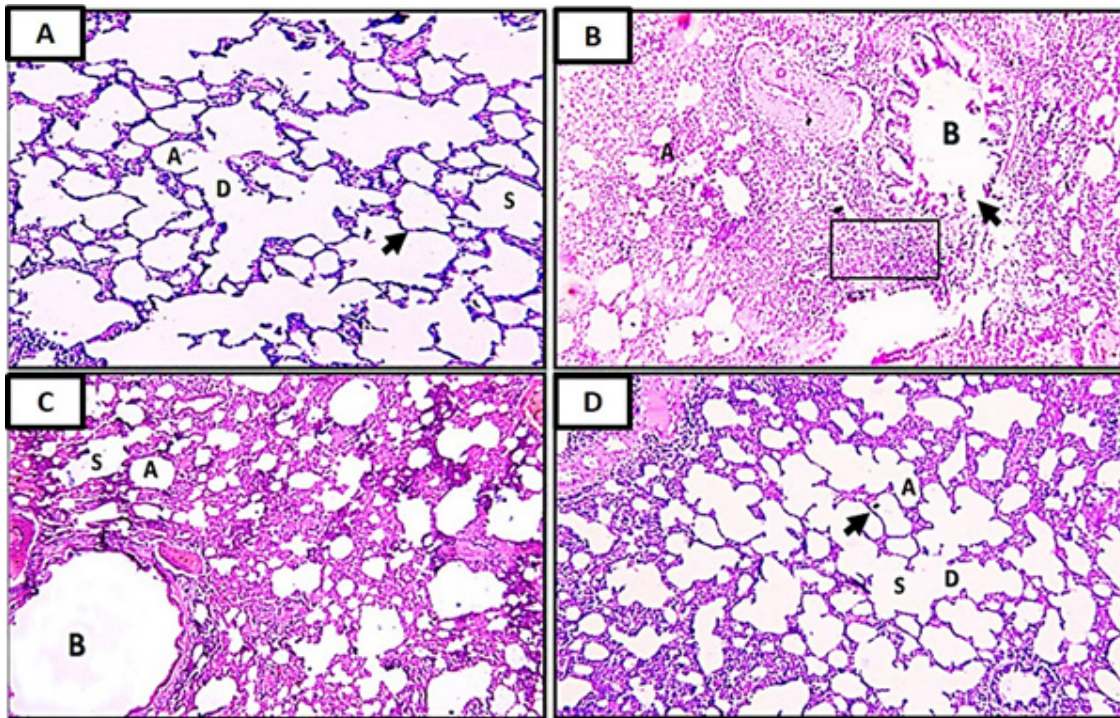
Fig. 1: A: showing lung tissue consisting of alveolar ducts (D), alveolar sacs(S) and terminal alveoli (A) with thin interalveolar septa in-between (black arrow). **B:** showing distorted alveolar walls (A) and bronchiolar walls (B) (black arrow) with mononuclear inflammatory cell infiltrate (the inset). **C:** showing apparent restoration of the most of the alveolar system; alveolar sacs (S) and alveoli(A). **D:** showing nearly normal alveolar ducts(D), sacs (S)and interalveolar septa (black arrow). (H&E, X100)
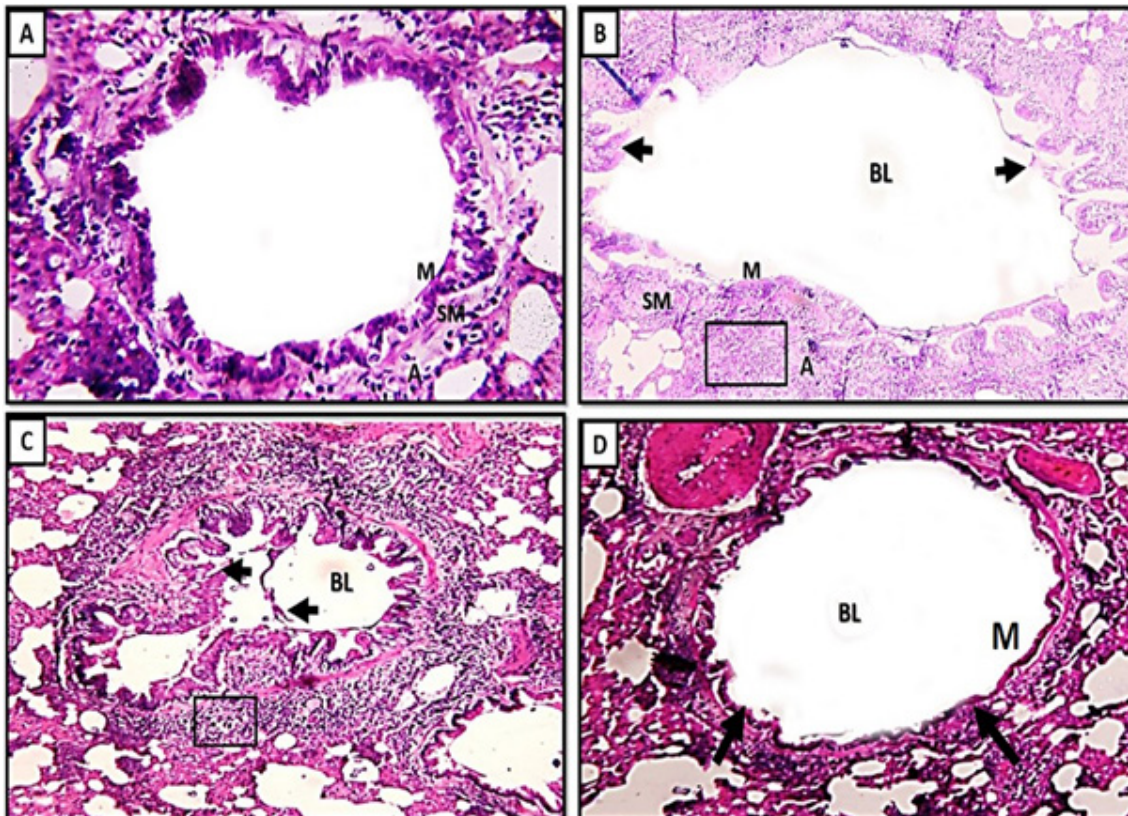
Fig. 2: A: showing the bronchiolar wall composed of mucosa(M), submucosa (SM) and adventitial layer (A). **B:** showing marked dilation of the bronchiolar lumen(BL) with distorted, sloughed epithelial lining (black arrows), the adventitial layer (A) appears blended with the pulmonary interstitium and invaded by inflammatory cell infiltrate(inset). **C:** showing some bronchioles with distorted epithelium (black arrows) and inflammatory cell recruitments appear around their wall (the inset). **D:** showing intact bronchiolar wall with intact epithelial lining. No sloughed debris inside the bronchiolar lumen and no inflammatory cell infiltrate in the submucosal layer (black arrows) (H&E, X100).
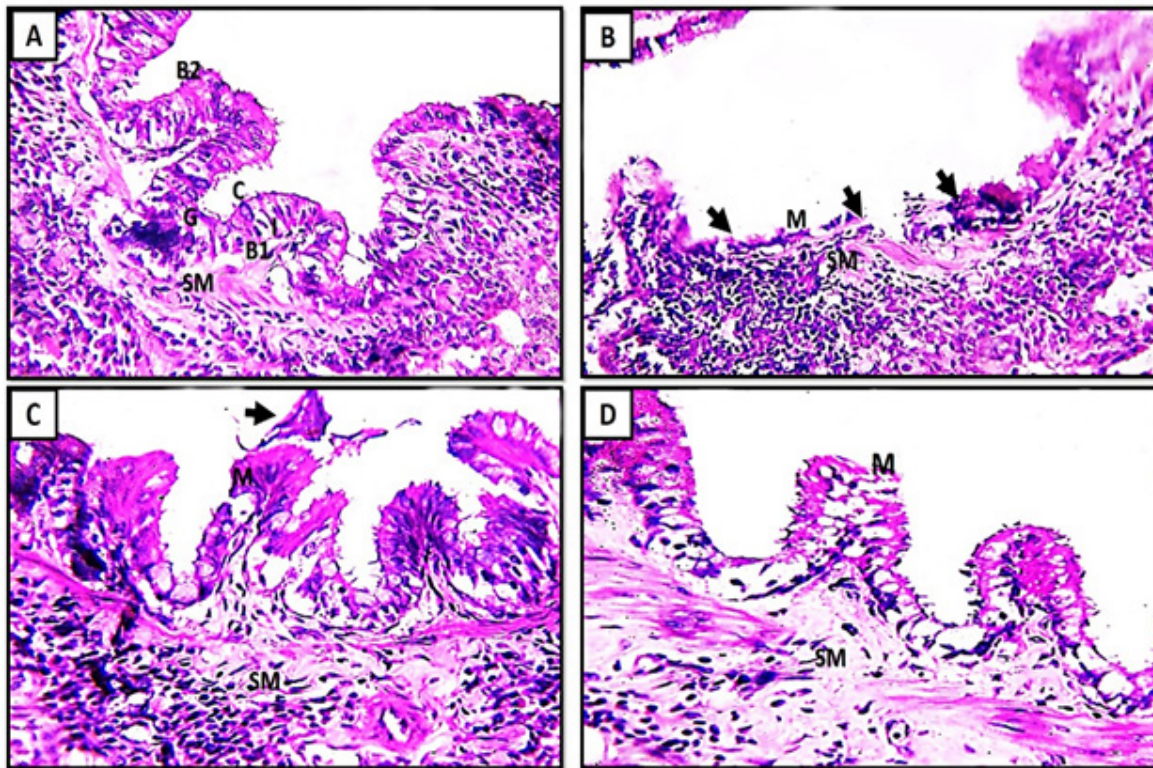
Fig. 3: A: showing the normal epithelial lining of the bronchiolar wall composed of basal cells(B1),intermediate cells(I),Clara cells with dome shaped surface and apical microvilli(C),goblet cells(G) and brush cells(B2). **B:** the epithelial lining of the bronchiolar mucosa appears markedly distorted down to the level of the basement membrane (black arrows) with extensive inflammatory cell infiltrate of the submucosal layer(SM). **C:** apparent restoration of the normal epithelial lining of the bronchiolar mucosa with sloughed debris inside the bronchiolar lumen(black arrow) and moderate reduction of the inflammatory cell infiltrate to the submucosal layer(SM). **D:** the bronchus appears with intact wall and intact mucosal epithelial lining with no sloughed debris inside the bronchial lumen and very mild inflammatory cell infiltrate of the submucosal layer(SM)(H&EX400).
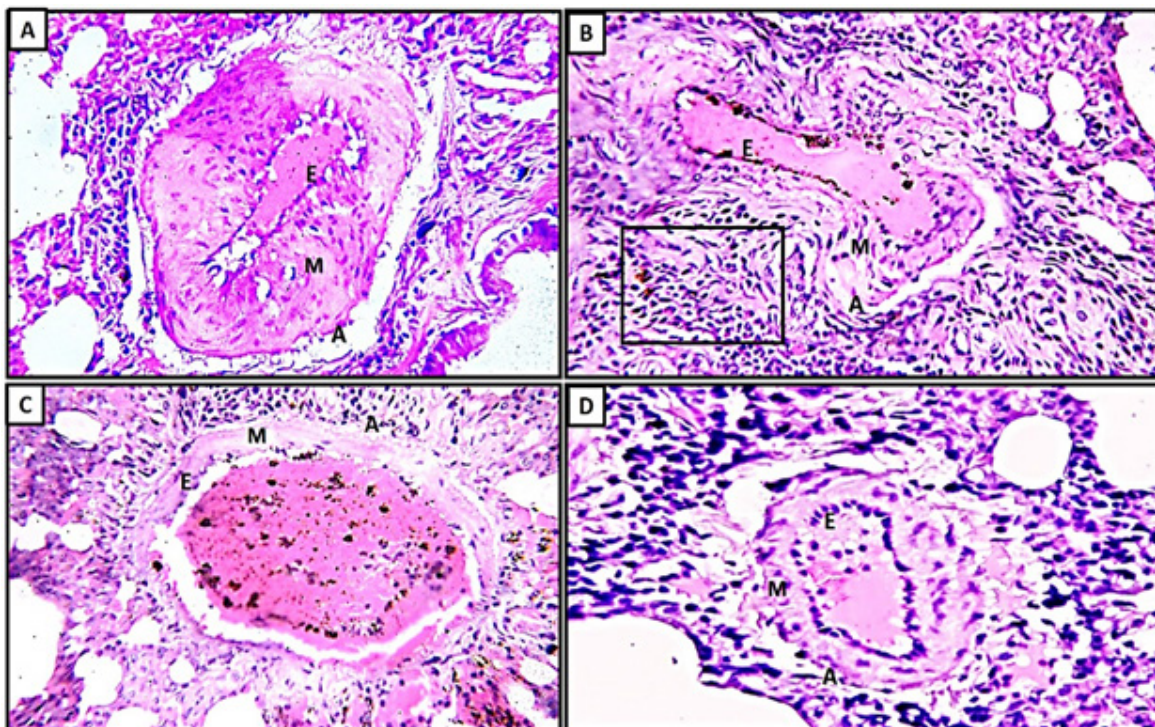

Fig. 4: A: showing the pulmonary blood vessels composed of intact endothelial lining (E), tunica media(M) and adventitial layer(A). **B:** the blood vessels appear markedly engorged, dilated with distorted endothelial lining (E),marked thinning of the tunica media (M)and adventitial layer(A).Note; the inflammatory cell infiltrate around the blood vessel(the inset). **C:** the blood vessels appear dilated, engorged with distorted endothelial lining but with normal appearance of both tunica media(M) and adventitial layer(A). **D:** remarkable restoration of the normal structure of the blood vessel wall with its different layers (H&E, X400).
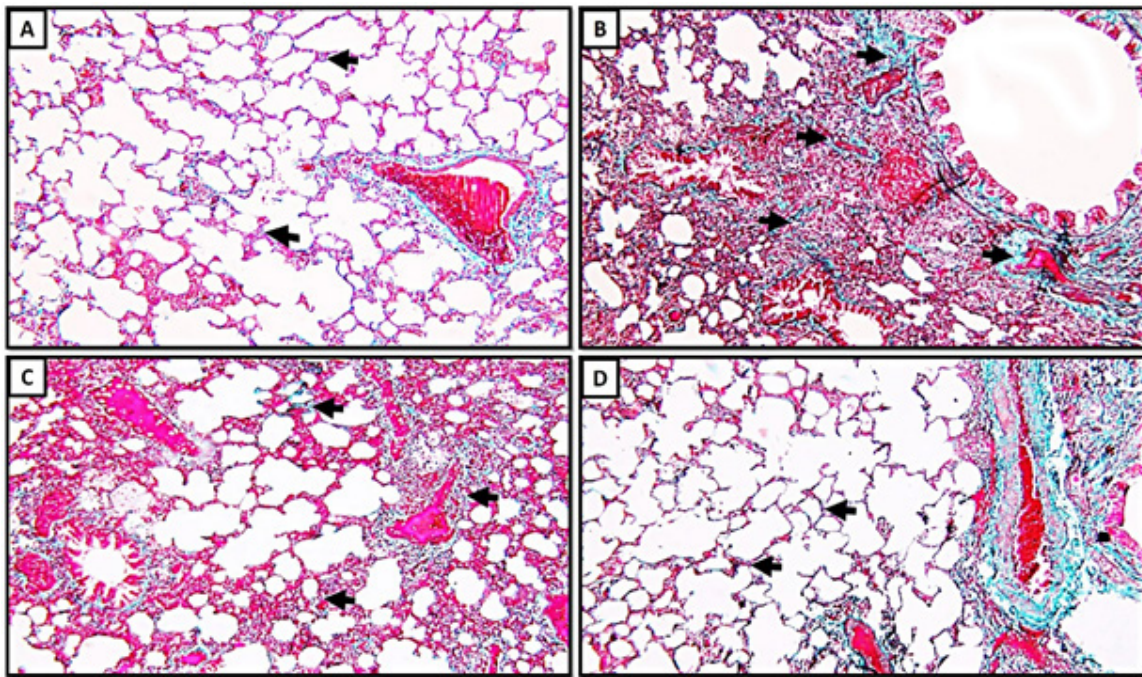
Fig. 5: A: showing collagen distribution of the pulmonary interstitium and interalveolar septa (black arrows). **B:** intense collagen deposition in the interalveolar septa, bronchiolar walls and around minor blood vessels (black arrows). **C:** showing moderate collagen distribution in the pulmonary parenchyma. **D:** apparent restoration of the normal collagen deposition in the pulmonary interstitium. (Masson's trichrome, x100).
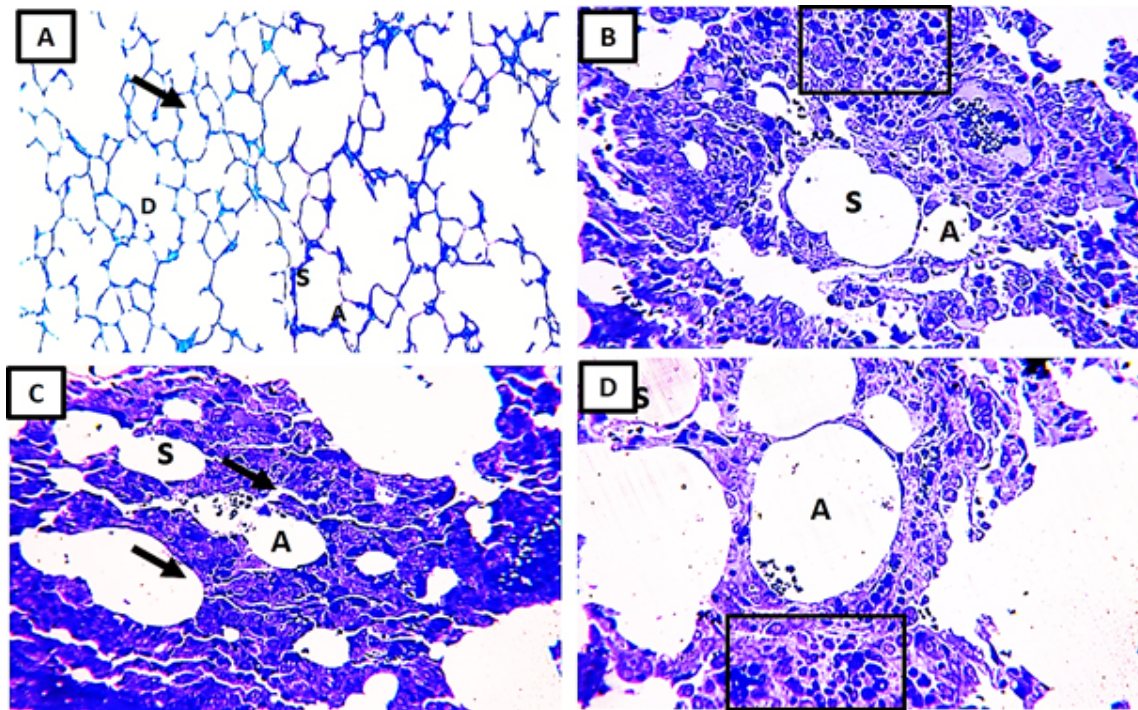

Fig. 6: A: showing the normal pulmonary architecture consisting of alveolar ducts(D), alveolar sacs(S) and alveoli(A). **B:** showing dilated alveoli(A) with extensive invasion of the mast cells to the pulmonary interstitium(inset). **C:** the mast cells still present in the pulmonary interstitium (black arrows). **D:** remarkable restoration of the alveolar system with marked reduction of mast cell infiltration (inset) (Toluidine blue, x400).
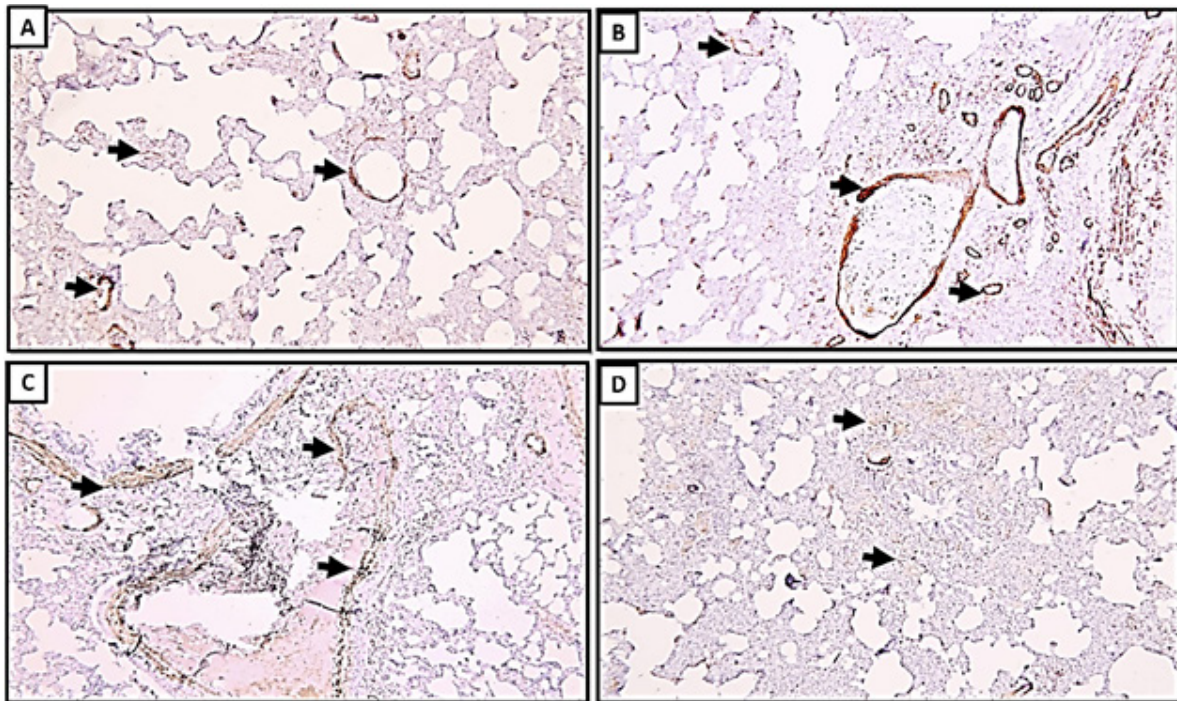
Fig. 7: A: showing very weak immune reaction to α-SMA. the reaction appears as mild brownish staining in the alveolar wall and the interalveolar septa (black arrows). **B:** showing strong positive immune reaction to α-SMA; appears as intense granular brownish staining in the alveolar septa(black arrows) and diffuse staining of the smooth muscles of the bronchial wall and blood vessels. **C:** moderate positive immune reaction to α-SMA in the interalveolar septa and in the bronchial wall (black arrows). **D:** mild immune reaction to α-SMA in the alveolar septa and the bronchial wall (black arrows) (α-SMA x 100).
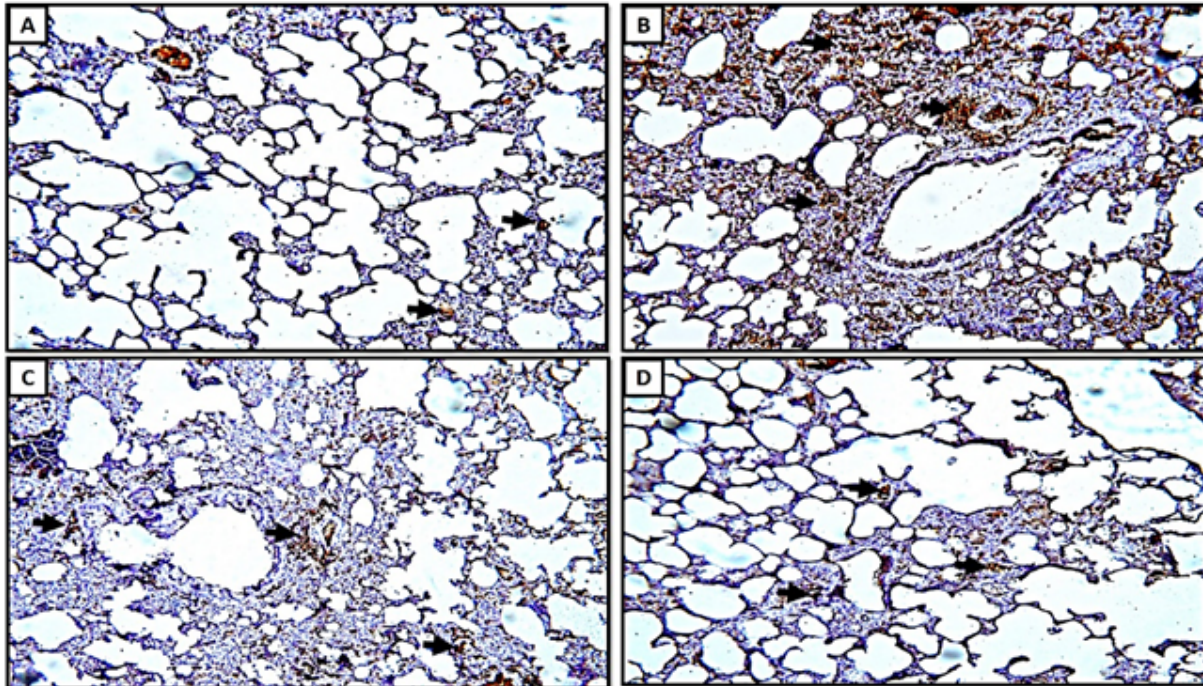

Fig. 8: A: showing very weak immune reaction to IL6, appears as mild brownish granular staining in the pulmonary parenchyma (black arrows). **B:** strong positive immune reaction to IL6 appears as intense brownish staining in the interalveolar septa (black arrows), surrounding the bronchial wall and blood vessels. **C:** moderate positive immune reaction to IL6 in the interalveolar septa. **D:** mild immune reaction to IL6 in the interalveolar septa (IL6 X100).
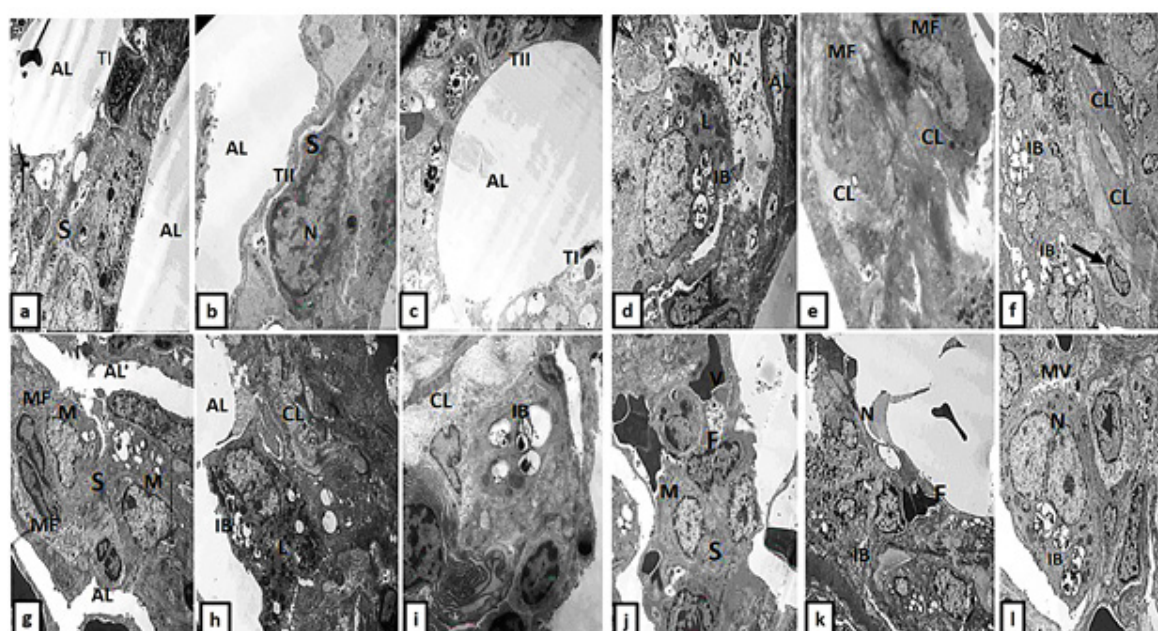
Fig. 9: a,b,c: showing patent alveolar lumen(AL) with thin interalveolar septum(S); the alveolar lumen lined with type I pneumocyte with euchromatic nucleus(TI)and typeII pneumocyte (TII)with hemogenus layer of surfactant near its luminal surface. **d, e, f:** showing ruptured pneumocyte and released micro particles in the alveolar lumen, multiple lysosomal bodies and inclusion bodies appeared near its luminal surface. Thickened alveolar septa(S), heavy collagen deposition(CL) and inflammatory cell infiltrate in the pulmonary interstitium (black arrows). **g, h, i:** showing thickened alveolar septa with myofibroblasts(MF) and macrophage(M) invading it. Heavy collagen deposition appeared in the pulmonary parenchyma and inclusion bodies in the cytoplasm of pneumocytes. **j, k, l:** showing patent alveolar lumen, the interalveolar septum still invaded by inflammatory cells, decreased number of inclusion bodies(IB), proliferating nuclei(N), apical microvilli(MV)and myofibroblasts(MF). (uranyl acetate X1000,25OO,1000,1500,15OO,1500,1500,1500,1500)

Table 1: illustrates area % of IL6 immunoreaction in the pulmonary interstitium

Group	Group I	Group II	Group III	Group IV
Mean area % of IL6 in lung	0.64	12.36	4.49	1.72
SD	0.09	1.14	0.88	0.23

Table 2: illustrates area % of α-SMA immunoreaction in the pulmonary interstitium

Group	Group I	Group II	Group III	Group IV
mean area % of α-SMA	0.33	4.65	1.59	0.88
SD	0.1	0.91	0.31	0.05

Table 3: illustrates area % of collagen immunoreaction in the pulmonary interstitium

Group	Group I	Group II	Group III	Group IV
Mean area % of collagen	1.73	13.84	8.21	4.79
SD	0.21	1.54	0.88	0.97

Table 4: illustrates serum level of IL6

| IL6 biochemistry	Group I (control)	Group II (Bleomycin)	Group III (Pirfenidone)	Group IV (Combined)	One Way ANOVA test		
	No. = 9	No. = 9	No. = 9	No. = 9	F	*P-value*	Sig.
Mean ± SD	34.36 ± 1.28	57.32 ± 3.04	48.85 ± 1.92	35.80 ± 1.41	70.500	<0.001	HS
Range	30.2 - 34.2	51.56 - 61.02	45.3 - 51.3	33.22 - 37.62			

Table 5: illustrates Serum level of SOD

| SOD biochemistry	Group I (control)	Group II (Bleomycin)	Group III (Pirfenidone)	Group IV (Combined)	One Way ANOVA test		
	No. = 9	No. = 9	No. = 9	No. = 9	F	*P-value*	Sig.
Mean ± SD	17.53 ± 2.04	29.80 ± 3.48	26.30 ± 3.07	19.29 ± 2.25	39.292	<0.001	HS
Range	15.2 - 21.6	25.84 - 36.72	22.8 - 32.4	16.72 - 23.76			

Table 6: illustrates serum level of MDA

| MDA biochemistry (U/ML)	Group I (control)	Group II (Bleomycin)	Group III (Pirfenidone)	Group IV (Combined)	One Way ANOVA test		
	No. = 9	No. = 9	No. = 9	No. = 9	F	*P-value*	Sig.
Mean ± SD	32.54 ± 1.28	57.32 ± 3.04	48.85 ± 1.92	35.80 ± 1.41	289.776	<0.001	HS
Range	30.2 ± 34.2	51.56 ± 61.02	45.3 ± 1.92	33.22 ± 37.62			

Table 7: illustrates serum level of TGβ

TGB biochemistry (PG/ML)	Group I (control)	Group II (Bleomycin)	Group III (Pirfenidone)	Group IV (Combined)	One Way ANOVA test		
	No. = 9	No. = 9	No. = 9	No. = 9	F	*P-value*	Sig.
Mean ± SD	5.44 ± 1.65	77.25 ± 23.38	16.32 ± 4.94	12.50 ± 3.80	67.531	<0.001	HS
Range	3.4 - 7.9	48.28 - 112.1	10.2 - 23.7	7.82 - 18.2			
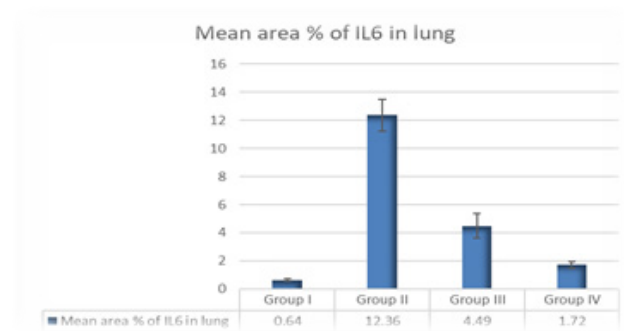
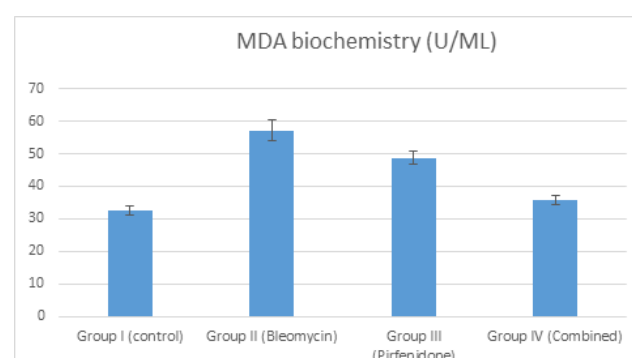**Histogram 1:** illustrates area % of IL6 immunoreaction in the pulmonary interstitium
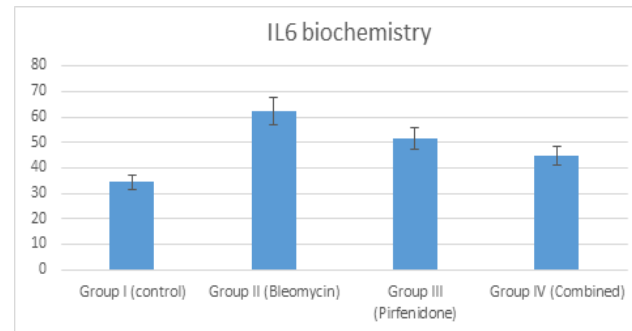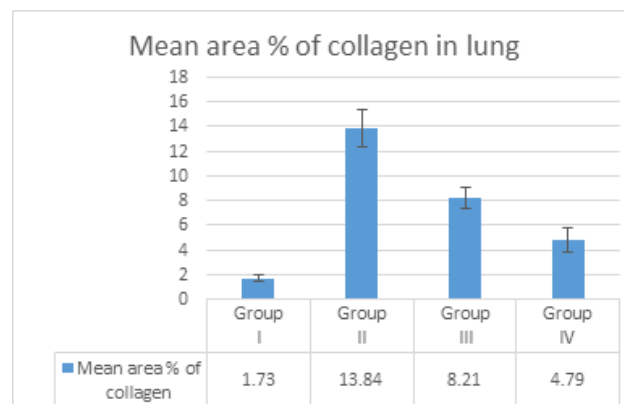

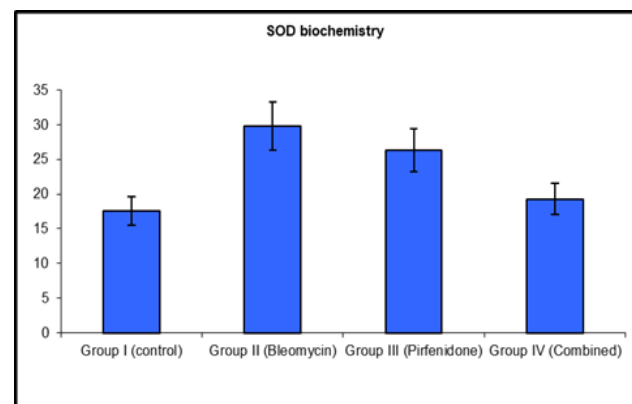**Histogram 4:** illustrates serum level of IL6
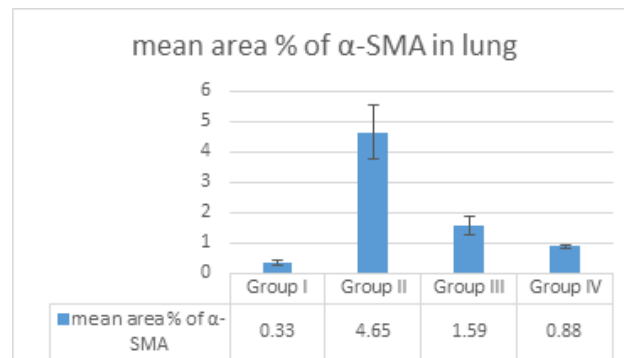
Histogram 2: illustrates area % of α-SMA immunoreaction in the pulmonary interstitium
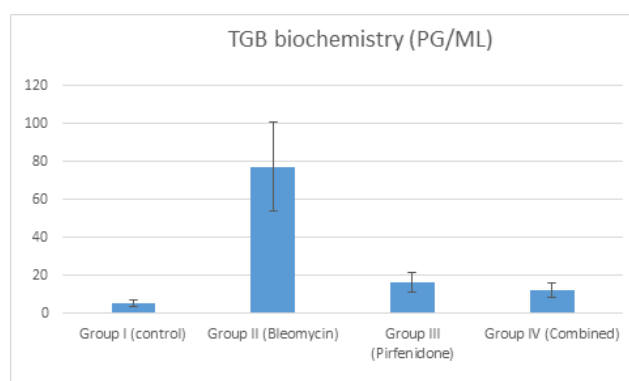

Histogram 5: illustrates Serum level of SOD

Histogram 3: illustrates area % of collagen immunoreaction in the pulmonary interstitium

Histogram 6: illustrates serum level of MDA

TGB biochemistry (PG/ML)

Histogram 7: illustrates serum level of TGβ

DISCUSSION

Percentage of patients who are still suffering from the complications of pulmonary fibrosis after COVID-19 pandemic are still increasing over time. Pulmonary fibrosis risk factors, histopathological characterization, and management remain poorly understood. As a result, there was a great argument about the different types of antifibrotic therapies that can decrease the florid inflammatory reaction which precedes the pulmonary fibrosis or protect against it[14]. Different protocols of management were applied. Previous clinical studies focused on the possible role of usage of single antifibrotic agent in treatment or the protection against pulmonary fibrosis[17,26,27].

The present study compared the efficacy of usage of single antifibrotic agent, pirfenidone against combined antifibrotic therapy colchicine and pirfenidone in the prophylaxis against pulmonary fibrosis. Moreover, the role of α-SMA, IL-6 and TGβ was analysed. The management of pulmonary fibrosis remains controversial, and a drug or drug combination that is optimal has not yet been identified[7].

In the current study, pulmonary fibrosis was induced by repeated intraperitoneal injections of bleomycin as described before in the methods. The presence of fibrosis was confirmed by the destruction of the normal architecture of the alveolar system, mononuclear inflammatory cell infiltrate and marked increase in the collagen deposition in the pulmonary parenchyma. In addition, there was marked increase in the expression of both α-SMA from the myofibroblasts which was markedly increased in the interalveolar septa, bronchial and smooth muscle blood vessels. A significant disruption of the normal alveolar architecture and an increase in extracellular matrix deposition were also observed. These findings are in agreement with previous experimental studies which proved that the myofibroblasts are the primary sources of type I collagen gene expression in the active fibrotic sites[6,13,31]. Moreover, the present study showed structural changes in both type I and II alveolar epithelial cells that was revealed by electron microscopy. Multiple type II alveolar cells showed some degenerative changes as empty lamellar bodies and loss of their apical microvilli. Zakaria et al., (2021)[29] reported that both types of alveolar lining epithelial cells are affected in BLM -induced interstitial pneumonitis but type I is more vulnerable to injury.

In the current wok, there was significant rise of both α-SMA, IL6 and collagen deposition in bleomycin treated group II. This could be attributed to the dramatic rise of the serum level of IL6 and TGβ which are a strong inflammatory cytokines indicating the presence of sever inflammatory reaction; this was in agreement with Zhao et al., (2014) &Shieh et al., (2019)[24,32]. Moreover, the presence of the mast cells which are specialized granulocytes that aid in the healing of wounds. Mediators derived from mast cells cause bronchoconstriction and mucosal edema. These cells are increasingly implicated in the pathophysiology of several airway disorders, including IPF. It has been demonstrated that mast cells enhance the migration and proliferation of fibroblasts. These cells can produce histamine and mast-specific proteases, which induce fibroblasts to secrete fibrogenic cytokines, hence encouraging fibrosis progression. According to (Pejler, 2020) & Reber et al., (2014)[18,20] mast cells and mast cell-specific chymase MCPT4 can mediate acute lung inflammation and injury in rats. In addition, elevated serum levels oxidative stress markers denoting for severe oxidative stress condition affecting the lung tissue and may contribute to the drastic histological changes which were observed in this group.

In the present study, Moderate improvement in the collagen distribution and decrease in the inflammatory cell infiltration were achieved by pirfenidone. Decreased recruitment of mast cells, collagen deposition but with persistent signs of degenerative changes on the alveolar lining cells and loss of apical microvilli. In addition, there was marked decrease in serum levels of both IL6 and TGβ indicating the improvement of the inflammatory condition. Moreover, there was decline in α-SMA expression from the myofibroblasts of the alveolar septa compared to the bleomycin treated group; this was proved by the significant statistical diminish in the expression of both α-SMA, IL6 and collagen deposition between pirfenidone treated group and bleomycin treated group II. Besides, obvious improvement in the oxidative stress condition that was confirmed by decline of serum levels of oxidative stress markers. Pirfenidone efficacy in treatment of pulmonary fibrosis in the animal models has already been determined and it is expected to be useful for the treatment of patients with idiopathic pulmonary fibrosis[9].

The best results were clearly shown in the combined group, there was an optimal improvement in the histopathological characteristics, marked decrease of both IL6, TGβ and α-SMA expression. In addition, there was marked decline of the serum inflammatory markers SOD, MDA. This confirms the strong anti-inflammatory and the antifibrotic proprieties of colchicine. From other point of view, its combination with pirfenidone may already enhanced its ability to control the drastic inflammatory and fibrosis condition. Previous researches proved Colchicine's anti-inflammatory properties through its

ability to inhibit polymorph nuclear leukocyte migration and phagocytosis[21].

Previous findings of Cumhur Cure et al., (2020)[5] documented that colchicine failed to inhibit or had a negligible effect on two cytokines that are believed to initiate the nonspecific inflammatory response, TNF-α and IL-6 production. Cumhur Cure et al., (2020)[5] reported that colchicine has an advantage over IL-6 inhibition, it acts upstream of the cytokine cascade and on other multiple cytokines[5]. Prabowo&Apriningsih (2021) reported that in rat models of bleomycin- and radiation-induced pulmonary fibrosis, colchicine has been shown to be an effective inhibitor of fibroblast proliferation and collagen synthesis. Additionally, it has been demonstrated that colchicine inhibits alveolar macrophage-derived growth factor and fibronectin and increases collagenase production. This makes colchicine a theoretically preferable candidate for a combined therapeutic strategy[19], this is in accordance with the results of the present study. Recent global trends emphasize the use of combined antifibrotic agents to treat post-COVID pulmonary fibrosis[11,15]. Multiple clinical trials are still needed to emphasize the results of the current investigation.

CONCLUSION AND RECOMMENDATIONS

In the present work, the antifibrotic anti-inflammatory and antioxidant effects of colchicine and pirfenidone were evaluated. The combined antifibrotic therapy offered a remarkable improvement in the architecture of the pulmonary tissue. There was a substantial improvement in the histopathological and immunohistochemical features in the combined group in comparison with pirfenidone treated group. According to the findings of this study, usage of combined antifibrotic therapy colchicine and pirfenidone as a protective agent in pulmonary fibrosis patients will greatly improve the inflammatory response and its complications and as a result; will improve the patients' symptoms and sequel of the disease.

CONFLICT OF INTERESTS

There are no conflicts of interest.

REFRENCES

1. Aburto M, Herráez I, Iturbe D, et al., (2018): Diagnosis of Idiopathic Pulmonary Fibrosis: Differential Diagnosis. Med. Sci. (Basel). Sep 4;6(3): p.73, indexed in PubMed: PMID: 30181506; PMCID: PMC6164303. doi: 10.3390/medsci6030073.

2. Angelidis C, Kotsialou Z, Kossyvakis C, et al., (2018): Colchicine Pharmacokinetics and Mechanism of Action. Curr. Pharm. Des. 2018;24(6):659-663. indexed in PubMed: PMID: 29359661. doi: 10.2174/1 381612824666180123110042,

3. Bagher M, Rosmark O, Elowsson Rendin L, et al., (2021): Crosstalk between Mast Cells and Lung Fibroblasts Is Modified by Alveolar Extracellular Matrix and Influences Epithelial Migration. Int. J. Mol. Sci. 2021 Jan 6;22(2):506, indexed in PubMed: PMID: 33419174; PMCID: PMC7825515. doi: 10.3390/ijms22020506.

4. Ballester B, Milara J, and Cortijo J., (2019): Idiopathic Pulmonary Fibrosis and Lung Cancer: Mechanisms and Molecular Targets. Int. J. Mol. Sci. Jan 30; 20(3): p.593, indexed in PubMed: PMID: 30704051; PMCID: PMC6387034. doi: 10.3390/ijms20030593.

5. Cumhur Cure M, Kucuk A, and Cure E., (2020): Colchicine may not be effective in COVID-19 infection; it may even be harmful? Clin. Rheumatol. 2020 Jul;39(7):2101-2102. Epub 2020 May 11, indexed in PubMed: PMID: 32394215; PMCID: PMC7213772. doi: 10.1007/s10067-020-05144-x.

6. Deng, J., Chen, P.P., Luo, M., et al., (2019): Inhibitory Effect of Total Ginsenoside on Pulmonary Fibrosis Induced by Bleomycin is involved in Matrix Metalloproteinase. The FASEB Journal, 33(S1): pp.681-1. https://doi.org/10.1096/fasebj.2019.33.1_supplement.681.1

7. Estebanez EB, Alconero LL, Fernández BJ, et al., (2021): The effectiveness of early colchicine administration in patients over 60 years old with high risk of developing severe pulmonary complications associated with coronavirus pneumonia SARS-CoV-2 (COVID-19): study protocol for an investigator-driven randomized controlled clinical trial in primary health care-COLCHICOVID study. Trials. 2021 Sep 6;22(1):590. indexed in PubMed: PMID: 34488841; PMCID: PMC8419390. doi: 10.1186/s13063-021-05544-7.

8. Ferrara F, Granata G, Pelliccia C, et al., (2020): The added value of pirfenidone to fight inflammation and fibrotic state induced by SARS-CoV-2: Anti-inflammatory and anti-fibrotic therapy could solve the lung complications of the infection? Eur. J. Clin. Pharmacol. Nov;76(11):1615-1618. Epub 2020 Jun 27, indexed in PubMed: PMID: 32594204; PMCID: PMC7320911. doi: 10.1007/s00228-020-02947-4.

9. Finnerty JP, Ponnuswamy A, Dutta P, et al., (2021): Efficacy of antifibrotic drugs, nintedanib and pirfenidone, in treatment of progressive pulmonary fibrosis in both idiopathic pulmonary fibrosis (IPF) and non-IPF: a systematic review and meta-analysis. BMC Pulm. Med. 2021 Dec 11;21(1):411. indexed in PubMed: PMID: 34895203; PMCID: PMC8666028. doi: 10.1186/s12890-021-01783-1.

10. George PM, Wells AU, Jenkins RG., (2020): Pulmonary fibrosis and COVID-19: the potential role for antifibrotic therapy. Lancet Respir. Med. 2020 Aug;8(8): p.807-815. Epub 2020 May 15, indexed in PubMed: PMID: 32422178; PMCID: PMC7228727. doi: 10.1016/S2213-2600(20)30225-3.

11. Hama Amin BJ, Kakamad FH, Ahmed GS, et al., (2022): Post COVID-19 pulmonary fibrosis; a meta-analysis study. Ann. Med. Surg. (Lond). 2022 May; 77:103590. Epub 2022 Apr 6, indexed in PubMed: PMID: 35411216; PMCID: PMC8983072. doi: 10.1016/j.amsu.2022.103590.

12. Kue, J. (2007): Electron microscopy methods and protocols. New Jersey. Springer. Science & Business Media 3:1-8. 2ND edition; edited by John Kuo.V.369; Chapter (2) processing biological tissues for ultrastructural study, pp:19-35.

13. Kolahian S, Fernandez IE, Eickelberg O, et al., (2016): Immune Mechanisms in Pulmonary Fibrosis. Am J Respir Cell Mol. Biol. 2016 Sep;55(3):309-22, indexed in PubMed: PMID: 27149613. doi: 10.1165/rcmb.2016-0121TR.

14. Meikle CKS, Creeden JF, Mc Cullumsmith C, et al., (2021): SSRIs: Applications in inflammatory lung disease and implications for COVID-19. Neuropsychopharmacol. Rep. 2021 Sep;41(3):325-335. Epub 2021 Jul 13, indexed in PubMed: PMID: 34254465; PMCID: PMC8411309. doi: 10.1002/npr2.12194.

15. Nathan, S.D., (2021): New Approaches in the Treatment and Management of Idiopathic Pulmonary Fibrosis. Millions of patients, treated as individuals., p.46. Epub ahead of print. doi:10.1007/s13311-020-00919-1.

16. Neighbors M, Cabanski CR, Ramalingam TR, et al., (2018): Prognostic and predictive biomarkers for patients with idiopathic pulmonary fibrosis treated with pirfenidone: post-hoc assessment of the CAPACITY and ASCEND trials. Lancet Respir. Med. 2018 Aug;6(8):615-626. Epub 2018 Jun 29, indexed in PubMed: PMID: 30072107. doi: 10.1016/S2213-2600(18)30185-1.

17. Oshitani N, Watanabe K, Sakuma T, et al., (2022): Tranilast, an antifibrotic agent and COVID-19-induced pulmonary fibrosis. QJM. 2022 Apr 20;115(4):249-250, indexed in PubMed: PMID: 35262694. doi: 10.1093/qjmed/hcac069.

18. Pejler G., (2020): Novel Insight into the in vivo Function of Mast Cell Chymase: Lessons from Knockouts and Inhibitors. J Innate Immun. 2020;12(5):357-372. Epub 2020 Jun 4, indexed in PubMed: PMID: 32498069; PMCID: PMC7506261. doi: 10.1159/000506985.

19. Prabowo, N.A. and Apriningsih, H., (2021): Colchicine reduces the degree of inflammation in COVID-19 patients. In IOP Conference Series: Earth and Environmental Science (Vol. 824, No. 1, p. 012087). IOP Publishing. doi: 10.1088/1755-1315/824/1/012087.

20. Reber LL, Daubeuf F, Pejler G, et al., (2014): Mast cells contribute to bleomycin-induced lung inflammation and injury in mice through a chymase/mast cell protease 4-dependent mechanism. J. Immunol. 2014 Feb 15;192(4):1847-54. Epub 2014 Jan 22. PMID: 24453258. doi: 10.4049/jimmunol.1300875.

21. Ribeiro SA, Lopes C, Amaral R, et al., (2020): The therapeutic potential of colchicine in the complications of COVID19. Could the immune metabolic properties of an old and cheap drug help? Metabolism. Open. 2020 Jul 21;7: 100045, indexed in PubMed: PMID: 32808940; PMCID: PMC7373059. doi: 10.1016/j.metop.2020.100045.

22. Schlesinger N, Firestein BL, and Brunetti L. (2020): Colchicine in COVID-19: An Old Drug, New Use. Curr. Pharmacol. Rep. 2020;6(4):137-145. Epub 2020 Jul 18, indexed in PubMed: PMID: 32837853; PMCID: PMC7367785. doi: 10.1007/s40495-020-00225-6.

23. She YX, Yu QY and Tang XX, (2021): Role of interleukins in the pathogenesis of pulmonary fibrosis. Cell Death Discover. 2021 Mar 15;7(1):52, indexed in PubMed: PMID: 33723241; PMCID: PMC7960958. doi: 10.1038/s41420-021-00437-9.

24. Shieh JM, Tseng HY, Jung F, et al., (2019): Elevation of IL-6 and IL-33 Levels in Serum Associated with Lung Fibrosis and Skeletal Muscle Wasting in a Bleomycin-Induced Lung Injury Mouse Model. Mediators Inflamm. 2019 Mar 27; 2019:7947596, indexed in PubMed: PMID: 31049028; PMCID: PMC6458868. doi: 10.1155/2019/7947596

25. Sim C, Lamanna E, Cirnigliaro F, et al., (2021): Beyond TGFβ1 - novel treatment strategies targeting lung fibrosis. Int. J Biochem. Cell Biol. Dec; 141:106090. Epub 2021 Oct 1, indexed in PubMed: PMID: 34601088. doi: 10.1016/j.biocel.2021.106090.

26. Singh, P., Behera, D., Gupta, S., et al., (2022): Nintedanib vs pirfenidone in the management of COVID-19 lung fibrosis: A single-centre study. Journal of the Royal College of Physicians of Edinburgh, p.14782715221103402. https://doi.org/10.1177/14782715221103402

27. Tanvir, M., Wagay, I., Nisar, S., et al., (2022): Early intervention with anti-fibrotic pirfenidone is effective than corticosteroids in preventing pulmonary fibrosis in severe COVID pneumonia patients. Current Medicine Research and Practice, 12(2): p.53. doi http://www.cmrpjournal.org IP: 182.64.241.156]

28. Wang J, Fang C, Wang S, et al., (2020): Danggui Buxue Tang ameliorates bleomycin-induced pulmonary fibrosis in rats through inhibiting transforming growth factor-β1/Smad3/ plasminogen activator inhibitor-1 signaling pathway. J Tradit Chin Med. 2020 Apr;40(2): p.236-244, indexed in PubMed: PMID: 32242389. https://doi.org/10.1155/2021/8030143.

29. Zakaria DM, Zahran NM, Arafa SAA, Mehanna RA, Abdel-Moneim RA. (2021): Histological and Physiological Studies of the Effect of Bone Marrow-Derived Mesenchymal Stem Cells on Bleomycin Induced Lung Fibrosis in Adult Albino Rats. Tissue Eng. Regen Med. 2021 Feb;18(1):127-141. Epub 2020 Oct 22. PMID: 33090319; PMCID: PMC7579902. doi: 10.1007/s13770-020-00294-0.

30. Zhang C, Wu Z, Li JW, et al., (2021): Discharge may not be the end of treatment: Pay attention to pulmonary fibrosis caused by severe COVID-19. J Med Virol. 2021 Mar;93(3):1378-1386. Epub 2020 Nov 1, indexed in PubMed: PMID: 33107641. doi: 10.1002/jmv.26634.

31. Zhang T, Zhou J, Yue H, et al., (2020): Glycogen synthase kinase-3β promotes radiation-induced lung fibrosis by regulating β-catenin/lin28 signaling network to determine type II alveolar stem cell trans differentiation state. FASEB J. 2020 Sep;34(9):12466-12480. Epub 2020 Jul 24, indexed in PubMed: PMID: 32706136. doi: 10.1096/fj.202001518.

32. Zhao H, Chan-Li Y, Collins SL, et al., (2014): Pulmonary delivery of docosahexaenoic acid mitigates bleomycin-induced pulmonary fibrosis. BMC Pulm Med. 2014 Apr 18; 14:64. indexed in PubMed: PMID: 24742272; PMCID: PMC3998951. doi: 10.1186/1471-2466-14-64.

الملخص العربى

الدور الوقائي المحتمل للبيرفينيدون مقابل العلاج المضاد للتليف الكولشيسين والبيرفينيدون في نموذج الفئران للتليف الرئوي الناجم عن البليوميسين وتقييم تأثيرهم المحتمل على TGFβ وα-SMA , IL6 (دراسة نسيجية وكيميائية مناعية)

ولاء عادل عبد المعز احمد

مدرس التشريح وعلم الاجنه- كليه الطب-جامعه عين شمس

مقدمه: تجذب استراتيجية العلاج بمضادات التليف الرئوي الانتباه في جميع أنحاء العالم خاصة بعد جائحة فيروس كورونا وما زالت تعد نقطة بحثيه حديثة.لذلك كان الهدف من هذه الدراسه توضيح الدورالوقائي المحتمل للبيرفينيدون فقط مقابل كلا من البيرفينيدون والكولشيسين مجتمعين في نموذج الفئران للتليف الرئوي الناجم عن البليوميسين.

الطرق و المواد المستخدمه: تم تقسيم أربعين من ذكور الجرذان البالغة بالتساوي إلى أربع مجموعات. المجموعة الضابطة الأولى. المجموعة الثانية المعالجة بالبليوميسين: (١٠ مجم / كجم / يوم عن طريق الحقن داخل الصفاق في الأيام الخمسة الأولى من التجربة). المجموعة الثالثة المعالجة بالبيرفينيدون: (١٠٠ مجم / كجم / يوم فموياً). والمجموعة المعالجة بكلا من الكولشيسين والبيرفينيدون: ١٠٠ مجم / كجم / يوم عن طريق الفم + كولشيسين ٠,٥ مجم / كجم / يوم عن طريق الفم لمدة ٣٠ يومًا).

النتائج: أظهرت النتائج النسيجيه للمجموعة الثانية حدوث تشوه ملحوظ في البطانة المخاطية للقصيبات الهوائية والجهاز السنخي. ظهرت الخلايا البدينة تتسلل إلى النسيج الخلالي الرئوي. ظهرت أجسام رقائقية متعددة في السيتوبلازم في النوع الأول والثاني من الخلايا الرئوية. علاوة على ذلك ، ظهرت الخلايا الليفية العضلية بأعداد كبيرة في الحواجز بين الحويصلات الهوائيه. كانت هناك زيادة ملحوظه في مناطق التلوين المناعي لكل من α-SMA و IL6 وترسب الكولاجين بين المجموعة الثانية والمجموعة الأولى. ارتفاع كبير في تركيزات TGβ و IL6 و MDA و SOD في الدم مقارنة بمجموعة التحكم. أظهرت المجموعة الثالثة تحسنًا معتدلًا في النتائج النسيجية المرضية والكيميائية المناعية وكذلك انخفاض ترسب الكولاجين وعلامات التهابات المصل بشكل ملحوظ بين المجموعتين الثالثة والثانية. لوحظت أفضل النتائج في المجموعة الرابعة ، انخفاض كبير في مناطق المناعة لكل من α-SMA و IL6 وانخفاض ملحوظ في مستويات المصل من SOD و MDA بين المجموعة الرابعة والمجموعتين الثالثة والثانية.

الخلاصة: قدم العلاج بمضادات التليف تحسنًا ملحوظًا في بنية النسيج الرئوي. كان هناك تحسن جوهري في الخصائص النسيجية المرضية والكيميائية المناعية في المجموعة المشتركة بالمقارنة مع المجموعة المعالجة ببيرفينيدون.